Available online at www.sciencedirect.com
ScienceDirect
C. R. Mecanique 336 (2008) 320–328
COMPTES RENDUS MECANIQUE
http://france.elsevier.com/direct/CRAS2B/

# A micromechanics-based non-local anisotropic model for unilateral damage in brittle materials

Qi-zhi Zhu, Jian-fu Shao, Djimedo Kondo *

*Laboratoire de mécanique de Lille-UMR CNRS 8107, Université de sciences et technologies Lille, cité scientifique, boulevard Paul-Langevin, 59655 Villeneuve d'Ascq cedex, France*

Received 8 February 2007; accepted after revision 16 October 2007

Presented by Jean-Baptiste Leblond

**Abstract**

The present Note is devoted to the formulation of a micromechanics-based model of non-local anisotropic damage and its application to concrete materials and structures. We first formulate a local anisotropic unilateral damage model on the basis of a suitable homogenization scheme which takes into account interactions between penny-shaped microcracks as well as their spatial distribution. The damage surface is built by using an energy release rate-based criterion. Then a non-local extension of the model is proposed by replacing the local energy release-rate for each family of microcracks by its average over a characteristic volume $V$ of the material centered at a given point. In order to demonstrate the efficiency of the non-local model in mesh-independent simulation of failure process in structures, some applications concerning failure of concrete materials and structures are presented. ***To cite this article: Q.-z. Zhu et al., C. R. Mecanique 336 (2008).***


**Résumé**

La présente Note est dédiée à la formulation d'un modèle micromécanique non local d'endommagement anisotrope ainsi qu'à son application aux matériaux et structures en béton. Nous formulons d'abord un modèle local d'endommagement unilatéral anisotrope en se basant sur un schéma d'homogénéisation adapté qui prend en compte l'interaction entre les microfissures ainsi que leur distribution spatiale. La surface d'endommagement est construite à l'aide d'un critère basé sur le taux de restitution de l'énergie. Une extension non locale du modèle est ensuite proposée en remplaçant le taux de restitution de l'énergie local associée à chaque famille de microfissures par sa moyenne sur un volume caractéristique $V$ du materiau centré au point matériel. Afin d'illustrer l'efficacité du modèle non local, en particulier l'indépendence de ces prédictions vis-à-vis du maillage, on présente quelques exemples concernant le processus de rupture de matériaux et structures en béton. ***Pour citer cet article : Q.-z. Zhu et al., C. R. Mecanique 336 (2008).***


*Keywords:* Damage; Homogenization; Non-local damage; Induced anisotropy; Crack interactions; Unilateral effect

*Mots-clés :* Endommagement ; Homogénéisation ; Endommagement non local ; Anisotropie induite ; Interaction entre fissures ; Effets unilatéraux

* Corresponding author.
*E-mail addresses:* qizhi.zhu@polytech-lille1.fr (Q.-z. Zhu), jian-fu.shao@polytech-lille.fr (J.-f. Shao), kondo@univ-lille1.fr (D. Kondo).

1631-0721/$ – see front matter 
doi:10.1016/j.crme.2007.10.010

## 1. Introduction

Damage by nucleation and growth of microcracks is an essential mechanism of inelastic behavior and failure process in brittle materials. A number of phenomenological and multiscale damage models have been developed for this class of materials. Compared to phenomenological models, the micromechanical approach is able to take into account physical mechanisms involved in the damage process at the microscopic scale [1]. Therefore, with these models, it is easier than by phenomenological models to take into account some specific aspects such as induced anisotropy and unilateral effects due to microcracks closure [2–4]. Thanks to the significant progress in computing techniques, micromechanical damage models of brittle materials can be now used in analysis of engineering structures with reasonable cost (see, for instance, [5]). However, the local formulation of such existing micromechanical models limits strongly their domain of applicability. Indeed, the deterioration of mechanical properties due to microcrack-induced damage leads generally to material softening and material failure by strain localization. It is well known that the analysis of failure process using continuum models without material length induces ineluctable spurious mesh dependency.

When strain localization appears, the basic hypothesis of scale separation required for homogenization methods is no longer fulfilled and the standard micromechanical approach cannot regularize the model, even interaction between microcracks in the representative elementary volume is taken into account. However, it seems that there is a physical link between crack interaction and strain localization as discussed by [6]. Different micromechanics-based methods have been recently proposed for the regularization of ill-posed boundary value problems. For instance, Drugan and Willis [7] (see also [8]) succeeded in deriving a non-local constitutive law for materials with graded properties. As pointed out by Lorentz and Andrieux [9], this is facilitated by the fact that the interaction is given a priori. However, the task seems to be very difficult when the interaction between length scales results from the evolution of the macroscopic fields themselves, as for brittle damage localisation. Another possibility, which results in a macroscopic gradient damage model, consists to enhance the homogenization approach by accounting for gradient effects on the boundary of the representative elementary volume (see [10]). The common point of all these approaches is to result in the introduction of some characteristic length of microstructures in the macroscopic relations. A simple, but practical approach, followed by many authors in brittle damage mechanics, consists in introducing a length scale in phenomenological damage models. In this framework, the non-local formalism appears easy to implement as a regularization technique in computer codes. Even in this phenomenological context, few studies concern anisotropic damage of brittle materials (see, for instance, [11]).

The contribution of this Note is to apply the non-local formalism to a new micromechanics-based anisotropic damage model dedicated to brittle materials with unilateral effects. First, based on the homogenization procedure proposed by Ponte-Castañeda and Willis [12] adapted here to unilateral damage, we derive an anisotropic thermodynamically consistent damage model. A validation of this local model on the Willam's test [13] is shown. Then, an integral form is applied for the determination of non-local damage conjugated force. Finally, the proposed non-local damage model is applied to two typical boundary values problems including a cement-based materials structure for which experimental data are available. The results obtained clearly show the efficiency of the proposed model in predicting basic mechanical behavior of brittle materials and in analysing the behavior of concrete structures. Comparisons with experimental data are provided.

## 2. Linear homogenization methods applied to materials containing interacting microcracks

Consider a representative elementary volume (r.e.v.), occupying a domain $\Omega$ and having a boundary surface $\partial\Omega$. This r.e.v., viewed as a matrix-inclusion system, is made up of a solid matrix with elasticity tensor $\mathbb{C}^s$ and of inclusions whose elasticity tensor is denoted $\mathbb{C}^r$, $r = 1, \ldots, N$. The local behavior is then characterized by: $\boldsymbol{\sigma}(\underline{z}) = \mathbb{C}(\underline{z}) : \boldsymbol{\varepsilon}(\underline{z})$ ($\forall \underline{z} \in \Omega$) with $\boldsymbol{\sigma}(\underline{z})$ and $\boldsymbol{\varepsilon}(\underline{z})$ as the local stress and strain fields, respectively. By taking the average of the local strain over $\Omega$, the effective (homogenized) stiffness tensor takes the standard form:

$$\mathbb{C}^{\text{hom}} = \mathbb{C}^s + \sum_{r=1}^{N} \varphi^r (\mathbb{C}^r - \mathbb{C}^s) : \mathbb{A}^r \tag{1}$$

where $\varphi^r$ is the volume fraction of the inclusions $r$. $\mathbb{A}^r$ is the so-called strain concentration tensor which relates in a linear way the local strain $\boldsymbol{\varepsilon}$ to the macroscopic uniform strain $\boldsymbol{E}$.

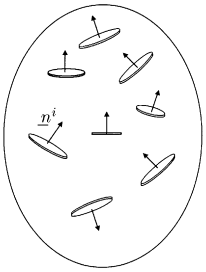


Fig. 1. R.e.v. of the microcracked material.

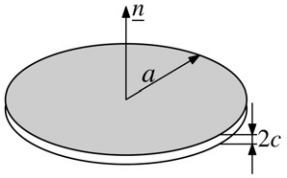


Fig. 2. A penny-shaped crack. The aspect ratio is $\epsilon = c/a$.

Obviously, the determination of the macroscopic stiffness tensor requires the computation of $\mathbb{A}^r$ which depends on the chosen homogenization scheme. Due to the possibility that it offers to take into account separately both the influences of the inclusions shape and their spatial distribution, the Ponte-Castañeda and Willis [12] scheme is adopted. The main results concerning the stiffness of the heterogeneous material predicted by this scheme is summarized in Appendix A.

We are interested now in adapting the above method to microcracked materials. A family of penny-shaped cracks can be approximated by a flat ellipsoid characterized by its unit normal vector (orientation) $\underline{n}$ and the aspect ratio $\epsilon = \frac{c}{a}$, with $a$ as the radius of the circular crack and $c$ as the half-length of the small axis (see Figs. 1 and 2).

It is convenient to express the volume fraction $\varphi^r$ of the $r$th cracks family in the form:

$$\varphi^r = \frac{4}{3}\pi a_r^2 c_r \mathcal{N}_r = \frac{4}{3}\pi \epsilon d^r \tag{2}$$

where $\mathcal{N}_r$ denotes the crack density (number of cracks per unit volume) of the family $r$, and $d^r = \mathcal{N}_r a_r^3$ (no summation) is the crack damage parameter widely used as internal variables in micromechanical analysis [15].

For open cracks, $\mathbb{C}^r$ is classically considered as $\mathbb{C}^r = 0$ so as to account for the cancellation of the stress on the crack faces. Following a methodology used by [14] for cracked materials, i.e. for low aspect ratios ($\epsilon \ll 1$), the fourth order tensor $\mathbb{C}^d$ in (A.5) can be determined for crack-like inclusions. The overall stiffness reads then:

$$\mathbb{C}^{\text{hom}} = \mathbb{C}^s - \sum_{j=1}^{N} d^r \mathbb{T}^r : \left( \mathbb{I} + \mathbb{P}_d : \sum_{j=1}^{N} d^r \mathbb{T}^r \right)^{-1} \tag{3}$$

where, still for open cracks and denoting $\mathbb{S}_\epsilon^r$ the Eshelby tensor associated with the $r$th crack family:

$$\mathbb{T}^r = \frac{4}{3}\pi \mathbb{C}^s : \lim_{\epsilon \to 0} \epsilon (\mathbb{I} - \mathbb{S}_\epsilon^r)^{-1} \tag{4}$$

By assuming a spherical spatial distribution for all cracks, $\mathbb{P}_d$ is given by (A.3). It must be noticed that due to directional character of the crack system, $\mathbb{C}^{\text{hom}}$ presents a priori a general anisotropy.

Note that the case of closed cracks is readily treated by considering a concept of fictitious closed crack stiffness $\mathbb{C}^r = k^s \mathbf{1} \otimes \mathbf{1}$ ($k^s$ is the bulk modulus of the solid matrix), as suggested in [14]. In this way, the proposed local model accounts for the unilateral effect due to microcrack closure.

## 3. Local and non-local formulations of the anisotropic damage model

### *3.1. The local micromechanics-based anisotropic damage model*

With the macroscopic free energy $W$ ($= \frac{1}{2}\boldsymbol{E} : \mathbb{C}^{\text{hom}} : \boldsymbol{E}$) in hand, the overall stress–strain relation:

$$\boldsymbol{\Sigma} = \frac{\partial W}{\partial \boldsymbol{E}} = \mathbb{C}^{\text{hom}} : \boldsymbol{E} \tag{5}$$

The strain energy release rate (conjugated force) associated with any damage variable $d^r$ is defined by:

$$F^{d^r} = \frac{1}{2}\boldsymbol{E} : \mathbb{T}^r : \boldsymbol{E} - \frac{1}{2}\boldsymbol{E} : (\mathbb{T}^r : \mathbb{B} : \mathbb{C}^d + \mathbb{C}^d : \mathbb{B} : \mathbb{T}^r) : \boldsymbol{E} + \frac{1}{2}\boldsymbol{E} : \mathbb{C}^d : \mathbb{B} : \mathbb{T}^r : \mathbb{B} : \mathbb{C}^d : \boldsymbol{E} \tag{6}$$

In the framework of thermodynamics of irreversible processes, the damage criterion should be determined as a function of the conjugated force $F^{d^r}$ on the basis of experimental evidences. However, the experimental identification of such a criterion is usually not easy. Noting that the expression of $F^{d^r}$ contains two linear terms in $\mathbb{T}^r$, $\mathbb{C}^d$ and $\mathbb{B}$, and one high order term, we propose to retain for the sake of simplicity as driving force for the damage process, only the two linear terms.

Denoting then by $\tilde{F}^{d^r}$ the contributions of the first two terms of (6), one has:

$$\tilde{F}^{d^r} = \frac{1}{2}\boldsymbol{E} : \mathbb{T}^r : \boldsymbol{E} - \frac{1}{2}\boldsymbol{E} : (\mathbb{T}^r : \mathbb{B} : \mathbb{C}^d + \mathbb{C}^d : \mathbb{B} : \mathbb{T}^r) : \boldsymbol{E} \tag{7}$$

The following simple damage criterion is proposed:

$$f^r(\tilde{F}^{d^r}, \underline{d}) = \tilde{F}^{d^r} - \mathcal{R}(d^r) \leqslant 0 \tag{8}$$

where $\mathcal{R}(d^r)$ is the local resistance against the damage propagation. Adapting a proposition of Marigo (1981) in the context of isotropic damage, a linear form, $\mathcal{R}(d^i) = c_0 + c_1 d^r$ is adopted in this work, with $c_0$ and $c_1$ two material constants. Combining this damage function with the normality rule, the evolution of the damage variables reads:

$$\dot{d}^r = \dot{\lambda}^{d^r} \frac{\partial f^r(\tilde{F}^{d^r}, d^r)}{\partial \tilde{F}^{d^r}} = \dot{\lambda}^{d^r}; \quad \dot{\lambda}^{d^r} \geqslant 0 \tag{9}$$

where the damage multipliers $\dot{\lambda}^{d^r}$ are determined by the consistency conditions $\dot{f}^r = 0,\ r = 1, \ldots, N$, for all families considered. The damage evolution being known, the rate form of the elastic damage law can then be deduced by following the standard procedure which consists of reporting all $\dot{d}^r$ in the differentiation of the stress–strain relation (5). A detail of the procedure can be found in [5].

### *3.2. Predictions of the anisotropic unilateral damage model for the Willam's test*

A very interesting case for concrete constitutive modeling is the so-called Willam's test [13]. This test is widely used to evaluate the capabilities of damage models to follow the rotation of the principal axes of the stress tensor. Although the test is purely theoretical, it has the merit of discriminating constitutive brittle damage laws and in particular to check their capacity to properly account for damage-induced anisotropy and microcrack closure effects. In this test, which has been a part of a benchmark (MECA) coordinated by EDF in France [16], the material is successively subjected to two loading steps in plane strain conditions.

- The first step is a uniaxial tension until the peak stress is reached. The components of the strain tensor in the plane $(\underline{e}_1, \underline{e}_2)$, $(E_{11}, E_{22}, E_{12})$, follow the path proportional to $(1, -\nu^s, 0)$ where $\nu^s$ is the Poisson ratio of the undamaged material; in the undamaged elastic regime, this corresponds to a uniaxial tensile loading in direction $\underline{e}_1$.
- The strain state obtained at the end of the first step is pursued by setting the increments of the strain tensor components $(E_{11}, E_{22}, E_{12})$ proportional to $(1, 0.5, 0.5)$. This loading step is equivalent to a biaxial extension accompanied by a sliding in the plane $(\underline{e}_1, \underline{e}_2)$; it induces a rotation of the principal axes of the strain tensor. The evolution of the major principal direction during this test is shown in Fig. 4 by means of $\theta_{\boldsymbol{E}}$ (angle between the principal direction of the macroscopic strain and the axis along $\underline{e}_1$).

The basic material properties proposed in [16] are as follows: Young modulus $E^s = 3.2 \times 10^{-4}$ MPa, Poisson ratio $\nu^s = 0.2$, compressive strength $f_c = 38.3$ MPa, strain corresponding to peak stress $E_{fc} = 2 \times 10^{-3}$, tensile strength $f_t = 3.0$ MPa and fracture energy $G_f = 110\ \mathrm{J\,m^{-2}}$. In agreement with the characteristics of the material, the following values of the model parameters are adopted: $c_0 = 7.5 \times 10^{-4}\ \mathrm{J\,m^{-2}}$ and $c_1 = 0$. In the micromechanical damage model, an initial microcracking state is implicitly assumed. The amount of this initial state must be in principle obtained from experimental observations. Due to the lack of such data, a scalar low value of $d_0 = 0.01$ is considered for the initial crack density parameter.

The results predicted by the micromechanical model for the Willam's test, $\Sigma_{11}$, $\Sigma_{22}$, $\Sigma_{12}$ as function of the axial strain $E_{11}$, are illustrated in Fig. 3. For comparison purpose, the uniaxial tensile stress–strain response is also provided. Due to the lack of experimental data for this test, we are interested in the qualitative response as it has been reported by other authors. The following comments can be made on the mechanical response in the damage regime:

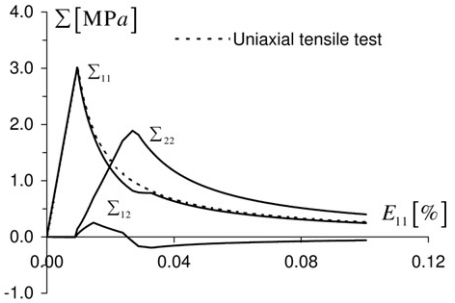


Fig. 3. Willam's test: in-plane stress components.

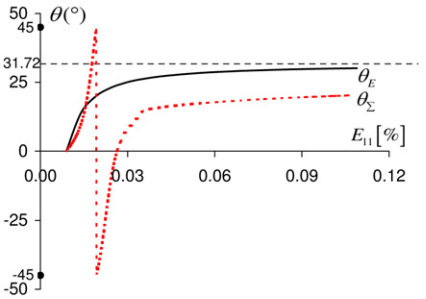


Fig. 4. Willam's test: evolutions of the angles between $\underline{e}_1$-axis and major principal directions of $\boldsymbol{\Sigma}$ and $\boldsymbol{E}$.

– For axial stress $\Sigma_{11}$, a softening behavior similar to the uniaxial tensile case is observed. During this softening phase, a slight plateau (or second peak) occurs at an axial strain near 0.03%. This plateau is simultaneously observed for the stress component $\Sigma_{22}$. It is noted that the $\Sigma_{22}$–$E_{11}$ curve passes over that of $\Sigma_{11}$ and reaches a peak at $E_{11} = 0.03\%$.
– The shear stress $\Sigma_{12}$ is first positive and then increases and reaches a peak before decreasing towards a second negative peak.

The reader interested by more details on these predictions can refer to [5]. The specific features, expected in the Willam's test, may be interpreted in terms of the rotation of the principal axes of stresses. Fig. 4 shows the comparison between the evolutions of the major principal stress direction $\theta_{\boldsymbol{\Sigma}}$ and the similar $\theta_{\boldsymbol{E}}$ for the strain tensor. A non-monotonic evolution of the principal stress rotation is noted. The difference between the two curves is the signature of the damage-induced anisotropy. It is interesting to notice that for the MECA benchmark, numerous models, even anisotropic, were not able to describe these different aspects which are considered very essential for the Willam's test.

### *3.3. Non-local formulation of the anisotropic damage model*

As already underlined, the degradation of material by microcrack growth generally leads to a material softening linked to a strain localization. It is well known that modeling of this phenomena by means of continuum models without material length leads to spurious mesh dependency. The strain softening or damage-induced strength degradation can be localized into a band of zero thickness with paradoxical consequences of structural failure with zero energy dissipation. In order to overcome this shortcoming, various methods have been proposed. Among these, the so-called non-local approaches are widely used. The basic idea implemented in the present study consists in replacing the local damage force $\tilde{F}^{d^r}$ for any considered family by its average over a representative volume $V$ of the material centered at a given point [17]. The damage variable $d^r$ is then function of the non-local driving force $\overline{\tilde{F}^{d^r}}$ which will be defined as:

$$\overline{\tilde{F}^{d^r}}(x) = \int_V \varpi(x, y)\, \tilde{F}^{d^r}(y)\, \mathrm{d}V(y) \tag{10}$$

In Eq. (10), $\varpi(x, y)$ is a space weighting function which describes the mutual non-local interactions and depends only on the distance between the source point $x$ and the receiver point $y$. Mathematically, the normalization condition $\int_V \varpi(x, y)\, \mathrm{d}V = 1$ is required for a uniform field. In this study, we adopt the following widely-used weighting function,

$$\varpi(x, y) = \frac{\alpha(x, y)}{\int_V \alpha(x, y)\, \mathrm{d}V} \tag{11}$$

where $\alpha$ is the Gaussian function:

$$\alpha(x, y) = \exp\left(-\frac{\|x - y\|^2}{2l^2}\right) \tag{12}$$

with $l$ a material characteristic length which defines the size of interaction zone for failure processes.

## 4. Numerical applications of the non-local damage model

### 4.1. Bar in uniaxial tension

The first application concerns a one-dimensional bar subjected to uniaxial traction. The bar is of length 110 mm with a weak zone in the central 10 mm for triggering localization, as illustrated in Fig. 5. This central zone is weakened by a 10% reduction in the Young's modulus. The following material parameters are used: $E^s = 3.6 \times 10^4$ MPa, $\nu^s = 0.2$, $c_0 = 7.5 \times 10^{-3}$ J m$^{-2}$ and $c_1 = 1. \times 10^{-3}$ J m$^{-2}$. The numerical tests are controlled by displacement and performed on three different meshes of 44, 88 and 176 elements. The material characteristic length is chosen to be 20 mm for the non-local analysis.

The load–displacement relations for the three meshes are shown and compared in Fig. 6. It is observed that the non-local model predicts correctly material softening behavior independently of the mesh size. The load–displacement curve is qualitatively in agreement with most data available in brittle materials under uniaxial tension.

For the analysis of the damage field, it must be first recalled that in the proposed model, the damage-induced anisotropy is given by the distribution of crack density parameter $d(\underline{n})$. Even in the present case, the anisotropy is general and can be rigorously represented only through a rosette (polar) diagram $d(\underline{n})$ (see details in [5]). However, for illustration purpose, it is convenient to built a second order tensorial approximation $\boldsymbol{D}$ of the crack density parameter distribution. This tensor, obtained by an integration over the surface of the unit sphere $\mathcal{S}^2$, is defined as:

$$\boldsymbol{D} = \frac{1}{4\pi} \int_{\mathcal{S}^2} d(\underline{n})(\underline{n} \otimes \underline{n}) \, \mathrm{d}\mathcal{S} \tag{13}$$

We provide in Fig. 7 the distribution profiles along the bar of the two principal values of $\boldsymbol{D}$. Remarkably, a stationary maximum damage principal value is obtained inside the weak zone.

### 4.2. Hassanzadeh's direct tension test

The second numerical application of the proposed model concerns a direct tension test performed by Hassanzadeh on a four-side notched concrete sample [18]. The geometrical description of the notched sample and the loading condition are indicated in Fig. 8. The hypothesis of plane strain condition is adopted for the numerical analysis.

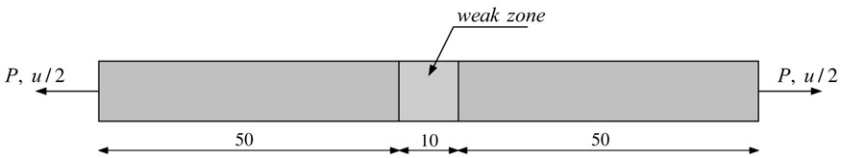


Fig. 5. Geometry (in mm) and loading condition of the bar in tension.

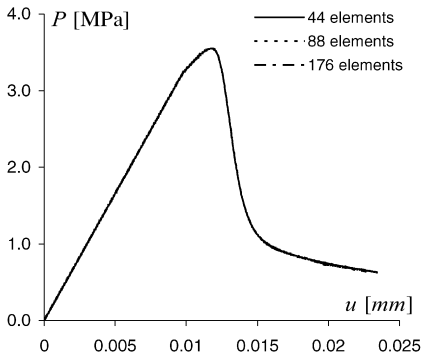


Fig. 6. Bar in tension: load–displacement response curves.

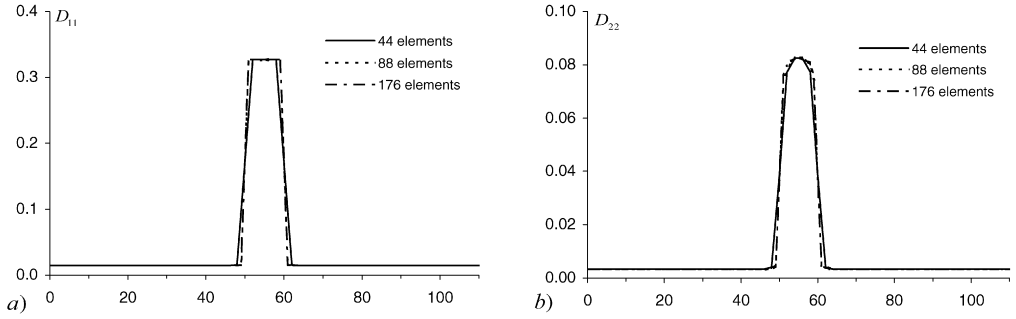


Fig. 7. Comparisons of damage distributions in the bar: (a) for $D_{11}$, and (b) for $D_{22}$.

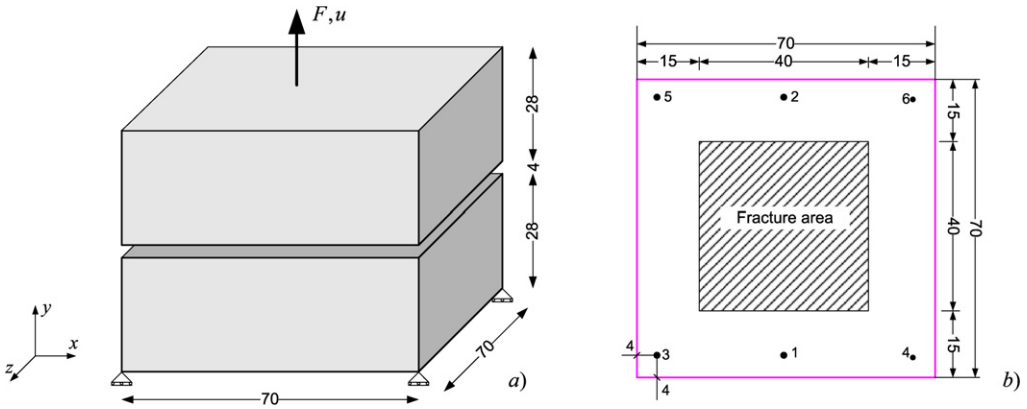


Fig. 8. Geometry (in mm) and loading condition of the Hassanzadeh test: (a) the structure; (b) the notch area.

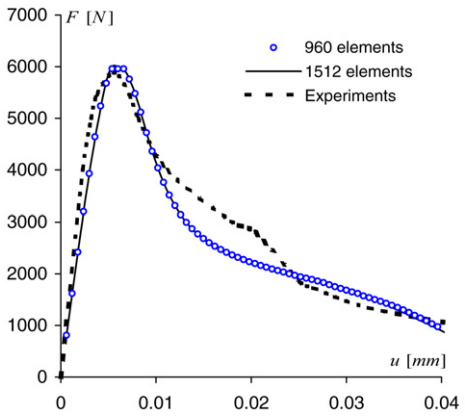


Fig. 9. Force–displacement response curves and comparisons to the experimental data reported in [18].

In order to study the mesh sensitivity of the proposed non-local micromechanics based model, two different meshes are considered: the first discretization with 960 rectangular elements and the second one with 1512 elements which is obtained by refining the discretization in the central fracture zone. The material constants and model parameters are those already given in Section 4.1.

Fig. 9 shows the force–displacement curves for the two meshes which are compared to the experimental data reported by Hassanzadeh [18]. A good agreement is observed between the numerical results and experimental data. The damage distributions at three different values of imposed displacements are presented and compared for the considered meshes in Figs. 10 and 11. The mesh independence of the numerical predictions is again observed.

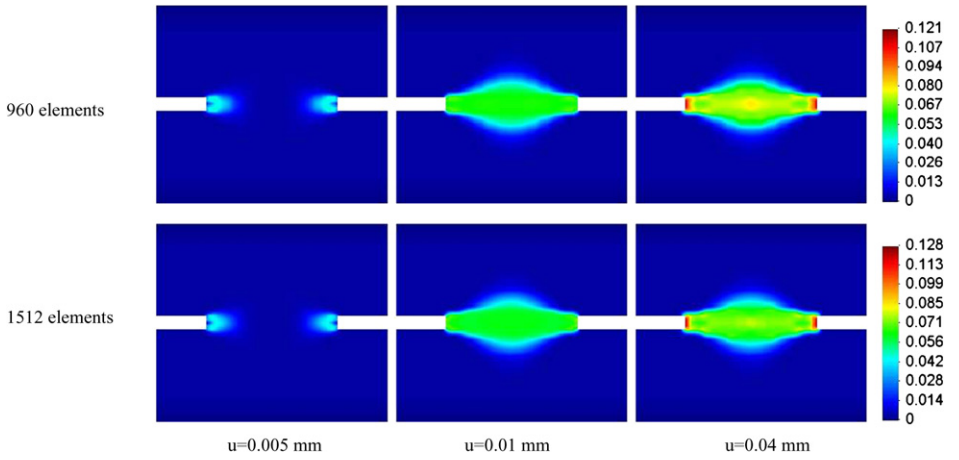


Fig. 10. Distributions of the damage component $D_{11}$ at three displacement levels for the two meshes.

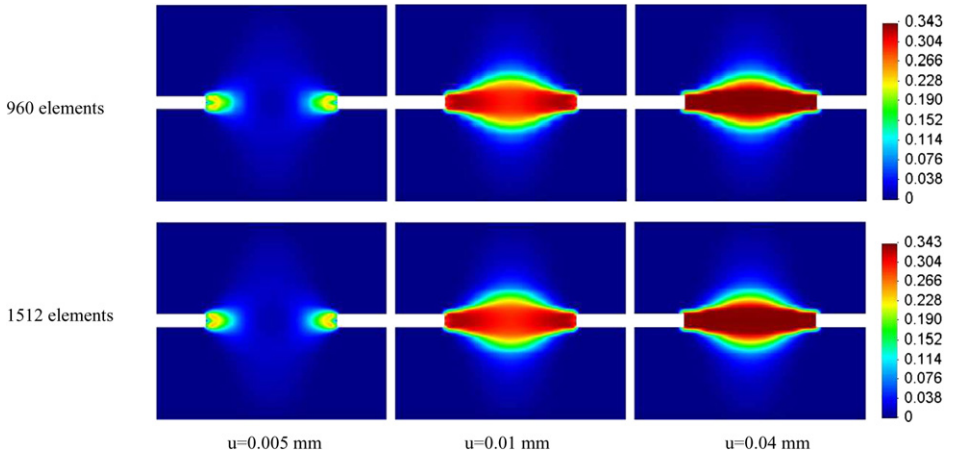


Fig. 11. Distributions of the damage component $D_{22}$ at three displacement levels for the two meshes.

## 5. Conclusions

In this study, we present a new homogenization-based non-local damage model for brittle materials. The micromechanical approach provides to the proposed model the capacity of dealing with main physical aspects of microcracking including anisotropic unilateral effects related to crack closure, interaction between microcracks, microcracks spatial distribution. It must be noticed that these features are generally neglected in widely-used macroscopic models. The proposed model contains a small number of parameters and can be easily implemented into computer code. Its extension to the non-local version allows us to model material softening and progressive failure process. The numerical applications show that the non-local model provides an efficient tool to analyze the mechanical deteriorating behaviors of concrete structures under complex loading conditions.

## Appendix A. Stiffness predicted by the Ponte-Castañeda and Willis [12] scheme

The corresponding overall stiffness tensor reads:

$$\mathbb{C}^{\text{hom}} = \mathbb{C}^s + \left( \mathbb{I} - \sum_{r=1}^{N} \varphi^r \mathbb{H}^r : \mathbb{P}_d \right)^{-1} : \sum_{r=1}^{N} \varphi^r \mathbb{H}^r \tag{A.1}$$

where

$$\mathbb{H}^r = \left[(\mathbb{C}^r - \mathbb{C}^s)^{-1} + \mathbb{P}^r_\epsilon\right]^{-1} \tag{A.2}$$

The fourth order tensors $\mathbb{P}^r_\epsilon$ and $\mathbb{P}_d$ are the Hill-type tensors, introduced in order to take into account the influences of the shape form of inclusions and of its spatial distribution respectively [12]. For simplicity, we adopt throughout this study a spherical spatial distribution for all inclusions; $\mathbb{P}_d$ reads then:

$$\mathbb{P}_d = \frac{\alpha}{3k^s}\mathbb{J} + \frac{\beta}{2\mu^s}\mathbb{K}; \quad \text{with } \alpha = \frac{3k^s}{3k^s + 4\mu^s};\ \beta = \frac{6(k^s + 2\mu^s)}{5(3k^s + 4\mu^s)} \tag{A.3}$$

(A.1) can be rewritten in the form (see [5]):

$$\mathbb{C}^{\text{hom}} = \mathbb{C}^s - \mathbb{C}^d : (\mathbb{I} + \mathbb{P}_d : \mathbb{C}^d)^{-1} \tag{A.4}$$

where, by using the Eshelby tensor ($\mathbb{S}_\epsilon = \mathbb{P}_\epsilon : \mathbb{C}^s$) [19]:

$$\mathbb{C}^d = \sum_{r=1}^{N} \varphi^r (\mathbb{C}^s - \mathbb{C}^r) : \left[\mathbb{I} - \mathbb{S}^r_\epsilon : \left(\mathbb{I} - (\mathbb{C}^s)^{-1} : \mathbb{C}^r\right)\right]^{-1} \tag{A.5}$$

For further simplifications, it is convenient to introduce $\mathbb{B} = (\mathbb{I} + \mathbb{P}_d : \mathbb{C}^d)^{-1} : \mathbb{P}_d$ and rewrite Eq. (A.4) in the form:

$$\mathbb{C}^{\text{hom}} = \mathbb{C}^s - \mathbb{C}^d + \mathbb{C}^d : \mathbb{B} : \mathbb{C}^d \tag{A.6}$$

## References


[1] D. Krajcinovic, Damage Mechanics, North-Holland, Amsterdam, The Netherlands, 1996.

[2] S. Andrieux, Y. Bamberger, J.J. Marigo, Un modèle de matériau microfissuré pour les roches et les bétons, Journal de Mécanique Théorique et Appliquée 5 (3) (1986) 471–513.

[3] L. Gambarotta, S. Lagomarsino, A microcrak damage model for brittle materials, International Journal of Solids and Structures 30 (2) (1993) 177–198.

[4] V. Pensée, D. Kondo, L. Dormieux, Micromechanical analysis of anisotropic damage in brittle materials, Journal of Engineering Mechanics, ASCE 128 (8) (2002) 889–897.

[5] Q.Z. Zhu, Applications des approches d'homogénéisation à la modélisation tridimensionnelle de l'endommagement des matériaux quasi fragiles : Formulations, validations et implémentations numériques, Ph.D. Thesis, University of Lille I, France, 2006 (in French).

[6] Z.P. Bazant, Nonlocal damage theory based on micromechanics of crack interactions, Journal of Engineering Mechanics, ASCE 120 (1994) 593–617.

[7] W.J. Drugan, J.R. Willis, A micromechanics-based nonlocal constitutive equation and estimates of representative volume element size for elastic composites, Journal of the Mechanics and Physics of Solids 44 (1996) 497–524.

[8] W.J. Drugan, Micromechanics-based variational estimates for a higher-order nonlocal constitutive equation and optimal choice of effective moduli for elastic composites, Journal of the Mechanics and Physics of Solids 48 (2000) 1359–1387.

[9] E. Lorentz, S. Andrieux, Analysis of non-local models through energetic formulations, International Journal of Solids and Structures 40 (2003) 2905–2936.

[10] M. Gologanu, J.-B. Leblond, G. Perrin, J. Devaux, Recent extensions of Gurson's model for porous ductile metals, in: P. Suquet (Ed.), Continuum Micromechanics, Springer, 1997, pp. 61–130.

[11] R. Desmorat, F. Gatuingt, F. Ragueneau, Nonlocal anisotropic damage model and related computational aspects for quasi-brittle materials, Engineering Fracture Mechanics (2007) 1539–1560.

[12] P. Ponte-Castañeda, J.R. Willis, The effect of spatial distribution on the behavior of composite materials and cracked media, Journal of the Mechanics and Physics of Solids 43 (1995) 1919–1951.

[13] K.J. Willam, E. Pramono, S. Sture, Fundamental issues of smeared crack models, in: S.P. Shah, S.E. Swartz (Eds.), SEM RILEM, Fracture of Concrete and Rock, Springer, New York, 1987, pp. 192–207.

[14] V. Deudé, L. Dormieux, D. Kondo, V. Pensée, Propriétés élastiques non linéaires d'un milieu mésofissuré, C. R. Mécanique 330 (2002) 587–592.

[15] B. Budiansky, J.R. O'Connel, Elastic moduli of a cracked solid, International Journal of Solids and Structures 12 (1976) 81–97.

[16] S. Ghavamian, I. Carol, A. Delaplace, Discussion over MECA projects results, Modèle de fissuration de béton, Revue française de Génie Civil 7 (5) (2003) 544–581.

[17] G. Pijaudier-Cabot, Z.P. Bazant, Nonlocal damage theory, Journal of Engineering Mechanics, ASCE 113 (10) (1987) 1512–1533.

[18] M. Hassanzadeh, Behavior of fracture process zones in concrete influenced by simultaneously applied normal and shear displacements, Ph.D. Thesis, Lund Institute of Technology, Lund, 1991.

[19] J.D. Eshelby, The determination of the elastic field of an ellipsoidal inclusion and related problems, Proceeding of the Royal Society of London, Series A 241 (1957) 375–396.